molecular pharmaceutics

ARTICLE

pubs.acs.org/molecularpharmaceutics

Comparison of Active and Passive Targeting of Docetaxel for Prostate Cancer Therapy by HPMA Copolymer−RGDfK Conjugates

Abhijit Ray,[†,‡,§] Nate Larson,[†,‡,§] Daniel B. Pike,[‡,∥] Michele Grüner,[†,‡,⊥] Sachin Naik,[†,‡,#] Hillevi Bauer,[†,‡] Alexander Malugin,[†,‡] Khaled Greish,[†,‡] and Hamidreza Ghandehari*[,†,‡,∥]

[†]Department of Pharmaceutics and Pharmaceutical Chemistry, [‡]Center for Nanomedicine, Nano Institute of Utah, and [∥]Department of Bioengineering, University of Utah, Salt Lake City, Utah, 84108, USA

[⊥]Johannes-Gutenberg-Universität Mainz, Mainz, Germany

[#]Pharmacy Department, The Maharaja Sayajirao University of Baroda, Gujarat, India

ABSTRACT: *N*-(2-Hydroxypropyl)methacrylamide (HPMA) copolymer−docetaxel−RGDfK conjugate was synthesized, characterized, and evaluated in vitro and in vivo in comparison with untargeted low and high molecular weight HPMA copolymer−docetaxel conjugates. The targeted conjugate was designed to have a hydrodynamic diameter below renal threshold to allow elimination post treatment. All conjugates demonstrated the ability to inhibit the growth of DU145 and PC3 human prostate cancer cells and the HUVEC at low nanomolar concentrations. The targeted conjugate showed active binding to $\alpha_v\beta_3$ integrins in both HUVEC and DU145 cells, whereas the untargeted conjugate demonstrated no evidence of specific binding. Efficacy at two concentrations (20 mg/kg and 40 mg/kg) was evaluated in nu/nu mice bearing DU145 tumor xenografts treated with a single dose of conjugates and compared with controls. RGDfK targeted and high molecular weight nontargeted conjugates exhibited the highest antitumor efficacy as evaluated by tumor regression. These results demonstrate that $\alpha_v\beta_3$ integrin targeted polymeric conjugates with improved water solubility, reduced toxicity and ease of elimination post treatment *in vivo* are promising candidates for prostate cancer therapy.

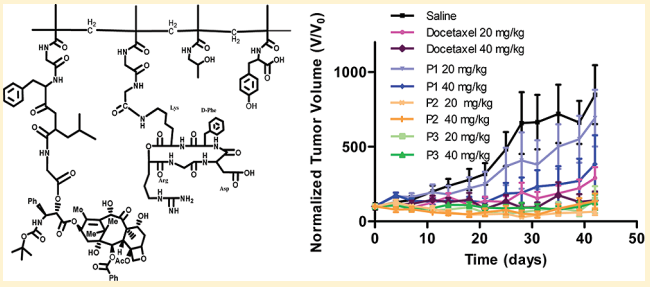

KEYWORDS: docetaxel, HPMA copolymer, prostate carcinoma, RGDfK, $\alpha_v\beta_3$ integrin, DU-145 prostate cancer cell line, PC3 prostate cancer cell line, targeted drug delivery

INTRODUCTION

Prostate cancer is the leading cause of cancer among men in the United States and the second leading cause of death with 217,730 new cases and an estimated 32,050 deaths in 2010.[1] In the past decade, much progress in the treatment of prostate cancer has been reported. However, routine treatment regimens have frequently changed due to poor prognosis of advanced disease. Despite standard treatment, the current survival from the time of diagnosis in patients with metastatic disease of 3.5 years is unacceptable.[2] These results demand the exploration of new alternatives which overcome drawbacks of current treatment modalities.

Docetaxel (Taxotere) is a semisynthetic natural product which was approved by the FDA in 2004 for metastatic and androgen dependent prostate cancer. Clinical trial results strongly suggest the use of docetaxel as a first line of treatment for prostate cancer.[3,4] Docetaxel binds to β-tubulin, thereby stabilizing microtubules and inducing cell-cycle arrest resulting in apoptosis.[5] It is up to five times more potent than paclitaxel in vitro with regard to tubulin promotion and inhibition of depolymerization.[6] There is incomplete cross resistance between paclitaxel and docetaxel, and they act synergistically with several drugs including cisplatin and carboplatin in cancer.[7] Docetaxel is reported to have both antiangiogenic and antitumor efficacy.[8] However, treatment with this drug is associated with gastrointestinal toxicity[9] and can result in aggravated risk of acute and subacute pulmonary damage.[10] Another major problem associated with administration of docetaxel is its poor aqueous solubility, requiring formulation with the nonionic surfactant polysorbate 80 (Tween 80). Administration of docetaxel is associated with the occurrence of unpredictable acute hypersensitivity reactions and cumulative fluid retention.[11] These adverse effects have been attributed, in part, to the presence of polysorbate 80 and have consequently initiated research focused on the development of a less-toxic, better-tolerated polysorbate 80-free formulation.

Considerable progress has been made over the past 2−3 decades in the development of polymeric carriers for targeted drug delivery to solid tumors.[12,13] Due to their macromolecular

Received: December 1, 2010
Accepted: May 20, 2011
Revised: April 20, 2011
Published: May 21, 2011

nature, polymeric systems accumulate passively in target tissues such as the reticuloendothelial system (RES) (through nonspecific uptake by macrophages) or tumors by a process called the enhanced permeability and retention (EPR) effect.[14,15] The mechanism of the EPR effect has been summarized according to the following cascade of events: (i) tumor angiogenesis results in hypervasculature, providing increased blood flow to the tumor; (ii) tumor vasculature becomes highly permeable for macromolecules and plasma proteins due to factors such as tumor vascular permeability factor, bradykinin, and tumor necrosis factor; (iii) a less effective functioning of lymphatic drainage observed in tumors results in long-term retention of macromolecular drugs. These factors result in larger carriers having decreased renal clearance, thereby taking longer to be eliminated from the body.[16]

HPMA copolymers are well characterized, water-soluble, biocompatible, nonimmunogenic and nontoxic synthetic polymeric drug carriers.[12,17,18] The in vivo disposition of macromolecules depends to a significant extent on their physicochemical properties. It has been shown that liver and kidney based clearance are the major factors affecting the biodistribution of macromolecules[19] and such clearance is a function of molecular weight. Studies have shown that HPMA copolymers and other polymeric macromolecules of molecular weights less than approximately 45 kDa (hydrodynamic diameter <5−6 nm) are rapidly filtered by the kidney.[16,20−22] Most macromolecules that passively target tumors via the EPR effect have sizes larger than 7 nm, in order to overcome the glomerular renal threshold, thereby resulting in prolonged plasma half-life. Despite significant progress made in the field of macromolecular drug delivery, one challenge encountered in the development of such therapy is the fate of large macromolecules post treatment.

Another challenge often overlooked while using the EPR effect as a rationale for drug delivery of macromolecules is the elevated interstitial fluid pressure (IVF) which reduces convective transport in the core of the tumor.[23,24] It is reported that the imbalance of the pro- and antiangiogenic factors leads to formation of chaotic new blood vessels in tumors.[25−27] This leads to uneven blood distribution, leaving unevenly perfused or unperfused regions inside the tumor.[28−31] These factors lead to interstitial hypertension in the core of the tumor.[32−34] Interstitial pressure and impaired blood supply reduce the effective transport of anticancer agents in solid tumors.[25] Active targeting can possibly overcome these limitations for drug penetration.[35]

The tripeptide sequence Arg-Gly-Asp (RGD) has been identified as a high affinity $\alpha_v\beta_3$ selective ligand by phage display.[36] The conformationally restrained cyclic RGDfK binds to $\alpha_v\beta_3$ up to 200-fold more avidly than linear peptides.[37] RGD peptides have been conjugated to humanized antibodies,[38] liposomes,[39−41] and poly(ethylene glycol)[42] to improve the biodistribution and increase tumor accumulation. The RGD (Arg-Gly-Asp) peptides have been used to target tumor angiogenesis.[43,44] They have been used for the targeted delivery of chemotherapeutic agents, gene therapy[45] and oncolytic adenovirus.[46] They have also been reported to be tumor penetrating, and its coadministration enhances the efficacy of anticancer drugs.[47] Compared to nontargeted systems, previous investigations in our laboratory[48−52] have identified actively targeted HPMA copolymer−cyclo-RGD conjugates that increase tumor accumulation. This accumulation takes place through specific interaction of RGD motifs present in the copolymer side chains with $\alpha_v\beta_3$ integrins overexpressed on both angiogenic blood vessels[37] and a variety of tumor cells including prostate cancer.[53] Enhanced accumulation was also demonstrated by active targeting in various human prostate cancer xenografts.[48,51] Further, these targeted conjugates have also been shown to inhibit HUVEC cell migration thereby delaying neoangiogenesis.[54] To enhance efficacy and reduce toxicity of docetaxel and to compare and contrast the effects of active vs passive targeting, our present study aims at producing HPMA copolymer−docetaxel−cyclic RGD conjugates for targeted delivery to prostate tumors.

METHODS

Chemicals. All chemicals obtained commercially were of analytical grade and used without further purification. Docetaxel was obtained from AK Scientific (Mountain View, CA). RGDfK (MW 604.5) was obtained from New England Peptide Inc. (Boston, MA) at >95% purity and used as supplied. Methacryloyl chloride, glycylglycine, and *p*-nitrophenol were obtained from Sigma-Aldrich (St. Louis, MO). Glycyl-phenylalanine and leucylglycine were obtained from Bachem Americas, Inc. (Torrance, CA). *N*-(2-Hydroxypropyl)methacrylamide (HPMA),[55] *N*-methacryloylglycylglycyl *p*-nitrophenyl ester (MA-GG-ONp),[56] *N*-methacryloylglycylphenylalanylleucylglycine (MA-GFLG-OH),[57] *N*-methacryloylglycylphenylalanylleucylglycine *p*-nitrophenyl ester (MA-GFLG-ONp),[57] and *N*-methacryloyltyrosinamide (MA-Tyr)[58] were synthesized and characterized according to previously described methods.

Synthesis and Characterization of Comonomers. N-Methacryloylglycylphenylalanylleucylglycyl−Docetaxel (MA-GFLG-Docetaxel). Docetaxel (0.335 g, 4.1 mmol), 4-(dimethylamino)-pyridine (DMAP, 0.049 g, 4.0 mmol) and MA-GFLG-OH (0.188 g, 4.0 mmol) were dried under vacuum. The reaction mixture was dissolved under nitrogen in anhydrous *N*,*N*-dimethylformamide (DMF, 5 mL) and cooled with an ice bath (salt/ice) at <0 °C, and diisopropylcarbodiimide (DIPC, 76 μL, 4.89 mmol) was added dropwise. The reaction mixture was subsequently stirred for an hour before the ice bath was removed; the mixture was allowed to warm up to room temperature and stirred overnight, and progress was monitored by thin layer chromatography (TLC, eluent dichloromethane (DCM):methanol (MeOH) (95:5)) for the disappearance of the starting material and the formation of MA-GFLG-docetaxel, and further characterized by mass spectroscopy (m/z $M^+ + Na = 1272.62$). DMF was removed under vacuum using a rotavapor. The product was purified by silica gel chromatography and eluted using ethyl acetate (EtOAc):MeOH (95:5). The product identity was confirmed by Thermo Finnegan LTQ FT high resolution mass spectrometry (m/z M^{+1} for $C_{66}H_{84}N_5O_{19}^+$, calculated 1250.57605 (100%), 1251.57941 (71.4%), found m/z 1250.57487 (100%), 1251.57827 (71.4%)).

N-Methacryloylglycylglycyl−RGDfK. MA-GG-ONp (0.20 g, 0.623 mmol) and RGDfK (0.376 g, 0.623 mmol) were mixed in a round-bottom flask, kept in a vacuum desiccator for 1 h followed by addition of anhydrous dimethyl sulfoxide (DMSO, 5 mL) and stirred for 18 h at room temperature. DIPEA (200 μL) was then added to the reaction mixture and further stirred for 4 h. The progress of the reaction was monitored by mass spectrometry for the disappearance of RGDfK (m/z M^{-1} 603.2) .The reaction mixture was concentrated under high vacuum, followed by addition of H_2O (25 mL). This mixture was partitioned in diethyl ether (3 × 25 mL). The organic layer was removed and the aqueous layer was lyophilized to obtain a white solid. Product formation was confirmed by Thermo Finnegan LTQ FT

Scheme 1. Schematic Synthesis and Resulting Structure of HPMA Copolymer−RGDfK−Docetaxel (P2) Conjugates[a]

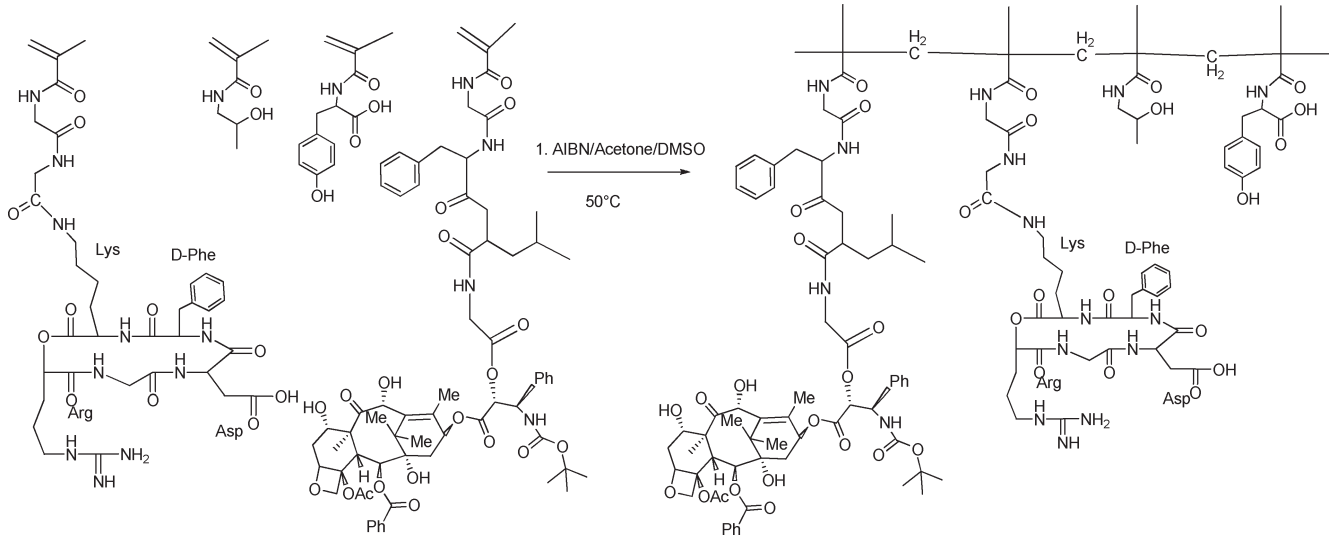

[a] Select copolymers contained the monocyclized RGDfK peptide targeting moiety to target docetaxel to $\alpha_v\beta_3$ integrins.

Table 1. Characteristics of HPMA Copolymer Conjugates

		comonomer feed composition (mol %)								wt %	
polymer no.	structure	HPMA	MA-GFLG-DOC	MA-GG-RGDfK	MA-Tyr	3-MPA	est M_w (kDa)[a] (SEC)	M_w/M_n[a]	hydrodynamic diameter (nm) (QELS)	DOC[b]	RGDfK[c]
P1	P-(GFLG-DC)	95.5	2.5		2	4	32.6	2.9	3.0	6.8	
P2	P-(GFLG-DC-RGDfK)	92.5	2.5	3	2	4	26.9	1.9	3.0	6.84	5.061
P3	P-(GFLG-DC)	95.5	2.5		2	1	87.1	4.9	7.6	7.15	

[a] Estimated by size exclusion chromatography (SEC). [b] Determined by HPLC. [c] Determined by amino acid analysis.

high resolution mass spectrometry (for $C_{35}H_{50}N_{10}O_{11}$, calculated m/z 786.36605 (100%), 787.36941 (37.9%), 788.37276 (7%), found m/z 786.38951 (100%), 787.39328 (37.9%), 788.39627 (7%)).

Synthesis and Characterization of HPMA Copolymer Conjugates. HPMA copolymers were synthesized via free radical copolymerization of comonomers in 10% v/v anhydrous DMSO in acetone using *N,N′*- azobisisobutyronitrile (AIBN) as the initiator (Scheme 1).[55] The feed composition of comonomers for all copolymers is given in Table 1. The weight composition of the comonomers to solvent was kept at 12.5:87.5 (w/w). The comonomer mixtures were sealed in an ampule under nitrogen and stirred at 50 °C for 24 h. Solvent was removed by rotary evaporation; copolymer precursor was dissolved in methanol, precipitated and washed in diethyl ether. Copolymer precipitates were dissolved in deionized water and purified using dialysis tube molecular weight cutoff (MWCO, 3500, SpectraPor) to remove small molecular weight impurities. Samples were characterized for weight average molecular weight (M_w), number average molecular weight (M_n) and polydispersity (M_w/M_n) by size exclusion chromatography (SEC) on a Superose 6 column (10 mm × 30 cm) (GE Healthcare, Piscataway, NJ) using a fast protein liquid chromatography (FPLC) system (GE Healthcare). The peaks that eluted off the column were monitored via ultraviolet absorbance (UV), differential refractive index (RI), and quasi-elastic light scattering (QELS) using a DAWN HELEOS II light scattering instrument (Wyatt Technologies, Santa Barbara, CA) with imbedded QELS and an OptiLab rEX differential refractometer (Wyatt Technologies). The Superose 6 column was previously calibrated with fractions of known molecular weight HPMA homopolymers. The hydrodynamic radii were determined by QELS and calculated from the Stokes−Einstein relation. All data were collected and analyzed using Wyatt Technology Corporation Astra 5.3.4.13 light scattering software (Wyatt Technologies).

Docetaxel and RGDfK Content Determination in Conjugates. Drug contents of the synthesized copolymers were determined by enzymatic release[59] of free docetaxel and quantification by HPLC. Briefly, 5.0 mg of the conjugate was dissolved in 200 μL of DMSO. Ten microliters of this solution was incubated in 20 μL of buffer A consisting of 0.1 M citrate phosphate buffer containing 2 mM EDTA at pH 6.0, 0.6 mM papain and 100 μL of buffer B consisting of 0.1 M citrate phosphate buffer containing 2 mM EDTA at pH 6.0 and 10 mM glutathione. The mixture was incubated at 37 °C for 24 h. The condition for complete release of the drug was optimized by varying the concentration of papain (0.1 mM to 1.0 mM) over time (data not shown). An aliquot (50 μL) of the reaction mixture was removed, diluted in 450 μL of water: acetonitrile (65:35), evaluated for docetaxel content by HPLC and compared to calibration standards prepared using serial dilutions of docetaxel in the mobile phase. Mobile phase consisted of deionized water (Milli-Q system, Millipore, Billerica, MA, USA) and HPLC grade acetonitrile (ACN) using the

following gradient: 0 min, 35% ACN; 15 min, 65% ACN; 25 min, 75% ACN; 30 min 95% ACN; 39 min, 100% ACN; 40 min 65% ACN. HPLC analyses were performed with an Agilent series 1100 HPLC (Agilent Technologies, Wilmington, DE, USA) equipped with an Alltima C18 5 μm 150 × 4.6 mm column and a photo diode array detector scanning at 200−500 nm. A flow rate of 1.0 mL/min was maintained, and the sample injection volume was 20 μL. A post time of 5 min was used to allow column equilibration between samples. UV absorbance at 230 nm was used for quantification of docetaxel. RGDfK content was determined by amino acid analysis (University of Utah Core Research Facilities, Salt Lake City, UT).

In Vitro Stability of the Conjugates. The rate of release of docetaxel from the polymer drug conjugates was evaluated in phosphate buffer saline (PBS) at pH 7.4 and in cell culture media. Two milligrams of each of the three copolymers P1, P2 and P3 (Table 1) was incubated in 1 mL of PBS (0.1 M phosphate buffer in 0.05 M of NaCl at pH7.4) and 1 mL of cell culture medium (recommended medium for DU145 from ATCC supplemented with 10% (v/v) fetal bovine serum (FBS) (HyClone, Logan, UT)), 100 U/mL penicillin, and 100 mg/mL streptomycin (Sigma). The samples were incubated at 37 °C, and a 100 μL aliquot was removed at times 0 min, 1 h, 2 h, 6 h, 12 h, and 24 h. The aliquots were immediately cooled to 4 °C in ice, and then free docetaxel was extracted with dichloromethane (DCM, 3 × 100 μL). The organic extract was concentrated under nitrogen (N_2) and then reconstituted in HPLC grade ACN:deionized water (Milli-Q system) (1:1). The release of the free drug was analyzed by HPLC and compared to calibration standards prepared using serial dilutions of docetaxel in the mobile phase. The mobile phase consisted of deionized water ((Milli-Q system) and HPLC grade ACN using the following gradient: 0 min, 50% ACN; 10 min, 50% ACN; 10.01 min, 95% ACN; 13 min 95% ACN; 13.01 min, 50% ACN; 15 min 65% ACN. HPLC analyses were performed with an Agilent series 1100 HPLC (Agilent Technologies, Wilimington, DE, USA) equipped with an Alltima C18 5 μm 150 × 4.6 mm column and a photo diode array detector scanning at 200−500 nm. A flow rate of 1.0 mL/min was maintained, and the sample injection volume was 20 μL. A post time of 2 min was used to allow column equilibration between samples. UV absorbance at 230 nm was used for quantification of docetaxel.

Cell Lines. Human umbilical vein endothelial cells (HUVEC) and human prostate cancer DU145 and PC3 cell lines were obtained from American Type Culture Collection (ATCC) (Manassas, VA). DU145 and PC3 cells were maintained in the recommended medium from ATCC supplemented with 10% (v/v) FBS, 100 U/mL penicillin, and 100 mg/mL streptomycin (Sigma). HUVECs were cultured in endothelial cell growth media-2 (EGM-2) (Lonza Inc., Allendale, NJ). Cells were incubated at 37 °C in a humidified atmosphere of 5% CO_2 (v/v) and kept in logarithmic phase of growth throughout all experiments.

In Vitro Cell Growth Inhibition. Cell number and growth kinetics were assessed by utilizing a water-soluble tetrazolium salt, WST-8 [2-(2-methoxy-4-nitrophenyl)-3-(4-nitrophenyl)-5-(2,4-disulfophenyl)-2*H*-tetrazolium, monosodium salt], as a component of Cell Counting Kit-8 from Dojindo Molecular Technologies, Inc. (Sunnyvale, CA). Cells were seeded in 100 μL of cultured medium at a density of 1×10^4 (DU145) or 1.5×10^4 (PC-3 and HUVEC) cells per cm^2 into a 96-well microtiter plate. They were subsequently allowed to adhere for 24 h before medium was replaced with fresh medium containing various concentrations of conjugates, free drug, or controls. Due to the poor water solubility of free docetaxel, stock solutions of conjugates, free drug, and controls were prepared in DMSO and subsequently diluted, resulting in a final concentration of 0.5% (v/v) DMSO in complete growth medium. No significant toxicities were observed for any cell line when exposed to 0.5% DMSO concentrations for the duration of the experiment. The cytotoxicity of free drug and HPMA copolymer−docetaxel conjugates was evaluated in two different experimental setups: (i) continuous incubation with drugs for 72 h (DU145, PC-3); (ii) short-term incubation or "pulse-chase" experiments where cells were incubated with drugs for 2 h only, washed with PBS and then incubated for an additional 70 h (DU145). In pulse-chase experiments all compounds were added to cells either immediately after dilution in cell growth medium or after 16 h of preincubation in the same medium at 37 °C. Following treatment with drugs, cells were washed once with PBS and WST-8 was added. The absorbance of colored product at 450 nm, reference at 630 nm, was measured using a SpectraMax M2 microplate reader (Molecular Devices, Sunnyvale, CA). The number of viable cells exposed to the drugs was expressed as a percentage of untreated (control) cells, concentration−response curves were graphed, and IC_{50} values were determined by nonlinear regression analysis using GraphPad Prism v. 5.03 (GraphPad Software Inc., La Jolla, CA).

Comparative Cell Receptor Binding Assay. The comparative affinities of free RGDfK and HPMA copolymer conjugates were assessed using a competitive binding assay to $\alpha_v\beta_3$ receptors present on HUVEC and DU145 cells. HUVEC and DU145 cells were harvested, washed with PBS, and resuspended in binding buffer (20 mmol/L tromethamine, pH 7.4, 150 mmol/L NaCl, 2 mmol/L $CaCl_2$, 1 mmol/L $MgCl_2$, 0.1% bovine serum albumin). Cell suspensions were added to 1.2 μm pore size 96-well Multiscreen HV filter plates (Millipore, Billerica, MA) at 100,000 cells per well. They were then coincubated at 4 °C with 0.5 ng of ^{125}I-echistatin (Perkin-Elmer, Waltham, MA) and increasing RGDfK peptide equivalent concentrations of copolymer conjugates or free RGDfK peptide between 0 and 500 μM. Following 20 min incubation, medium was removed from cells using a Multiscreen vacuum manifold (Millipore) and cells were washed three times with binding buffer. Filters were collected and radioactivity was determined using a Cobra auto-gamma-counter (Canberra Industries, Inc., Meriden, CT). Each experiment was performed in triplicate, with $n = 4$ per replicate. Binding percentage relative to control wells containing only ^{125}I-echistatin was calculated, and nonlinear regression analysis and determination of IC_{50} values was carried out using GraphPad Prism.

In Vivo Efficacy of HPMA Copolymer Drug Conjugates. Six-week-old athymic (nu/nu) mice were obtained from Charles River Laboratories (Davis, CA, USA) and used in accordance with the Institutional Animal Care and Use Committee (IACUC) of the University of Utah. Mice were anesthetized using 4% isoflurane mixed with oxygen followed by subcutaneous injection of 1×10^7 DU145 cells per flank ($n = 5$ mice per treatment group). When the mean tumor size had reached approximately 50 mm^3, the mice were treated with a single dose of conjugates, free docetaxel, or control (saline injection) via tail vein injection. Conjugates were prepared in saline, and free docetaxel required formulation in polysorbate 80:EtOH:saline (20:13:67, v/v/v) to ensure solubility. The animals were routinely monitored; tumor growth was measured twice weekly, and

tumor volume was calculated as length × width^2 × $\pi/6$. Tumor volumes at each time point were normalized by the initial volume and are reported as mean normalized tumor volume (%) ± standard error of the mean. Animal weights were also measured at each time point and normalized to initial animal weight reported as mean ± standard deviation.

Statistical Analysis. Differences in growth inhibition IC_{50} values were determined by one-way ANOVA. Where differences were detected, Scheffe's post hoc analysis was used to test for significance between groups. In vivo data was analyzed by repeated measure ANOVA. Where differences were detected, Scheffe's post hoc analysis was used to test for significance between groups. Graphpad Prism v. 5.03 and SPSS v 17 (Chicago, IL) were used for statistical analysis. The significance level was set at $\alpha = 0.05$ for all statistical tests.

RESULTS AND DISCUSSION

Physicochemical Characteristics of Polymeric Conjugates. The characteristics of the HPMA copolymer conjugates are listed in Table 1. The sizes of the copolymer conjugates, i.e., P1 (HPMA copolymer−GFLG−docetaxel (low molecular weight)), P2 (HPMA copolymer−GFLG−docetaxel−GG−RGDfK) and P3 (HPMA copolymer−GFLG−docetaxel (high molecular weight)) were controlled by changing the ratio of the total comonomers to 3-mercaptopropionic acid (3-MPA), which acts as a chain transfer reagent in the presence of a free radical initiator.[60] Docetaxel was attached to the HPMA copolymer backbone via a lysosomally degradable oligopeptide linker glycylphenylalanyl-leucylglycine, and targeting peptide RGDfK was attached by the nondegradable dipeptide glycylglycine. The P1 and P2 conjugates (with and without $\alpha_v\beta_3$ integrin targeting peptide RGDfK) had a 4% molar equivalent of 3-MPA, while the high molecular weight conjugate had a 1% molar equivalent of 3-MPA. SEC and HPLC profiles of the conjugates indicate the absence of small molecular weight impurities or free docetaxel. Drug content of each polymer was measured by releasing docetaxel enzymatically using papain followed by HPLC analysis and was found to be 6.8 wt %, 6.84 wt % and 7.15 wt % for P1, P2 and P3 respectively. The molecular weights of the copolymers as estimated by SEC on a Superose 6 column were 32.6 kDa, 26.9 kDa and 87.1 kDa. The hydrodynamic diameters of the conjugates as measured by quasi elastic light scattering (QELS) were 3.0 nm, 3.0 nm and 7.6 nm for P1, P2 and P3 respectively. RGDfK content of P2 was estimated by amino acid analysis and was found to be 5.061 wt % of the polymer.

In Vitro Stability of Polymer−Drug Conjugates. The in vitro stability of conjugates was investigated at physiological pH as well as in cell culture medium at pH 7.4. The three conjugates P1, P2 and P3 released 14.8 ± 2.6%, 18.6 ± 4.8% and 10.8 ± 2.3% in PBS pH 7.4 and 23.4 ± 3.3, 23.2 ± 2.4 and 24.1 ± 2.7 in cell culture medium in the first 24 h (Figure 1). The higher release of the conjugates in the medium is likely due to the presence of serum esterases which cleave the ester bond between the conjugate and the drug. All copolymer systems under study had less than 20% release of docetaxel in PBS at pH 7.4 and less than 25% release in cell culture medium in 24 h, indicating adequate stability for in vivo accumulation of a portion of intact conjugates in solid tumors.

In Vitro Cell Growth Inhibition. All conjugates inhibited proliferation of prostate cancer cell lines and HUVECs at nanomolar concentrations (Figure 2A−C). Analysis of growth

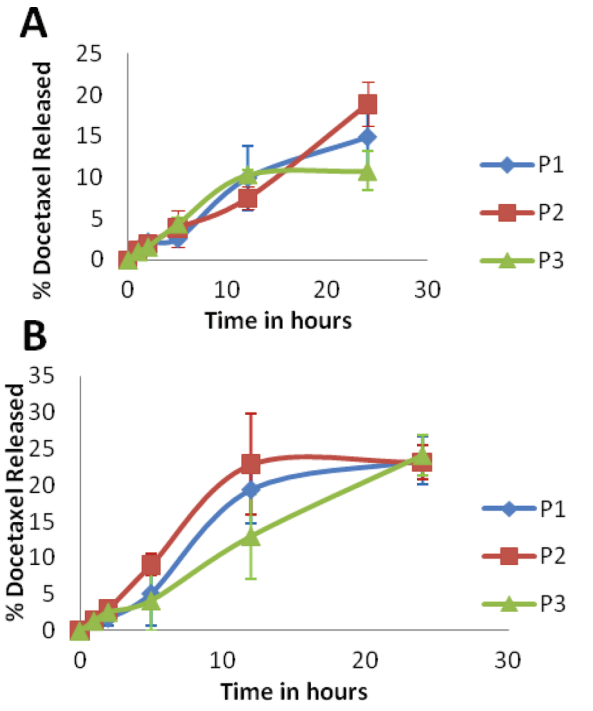

Figure 1. Stability of polymer−drug conjugates in PBS, pH 7.4 (A) and cell culture medium (B) at 37 °C. Diamond represents P1, the untargeted low molecular weight conjugates; the square represents P2, the RGDfK targeted low molecular weight conjugate; and the triangle represents P3, the high molecular weight conjugate. The values of 3 independent measurements are presented as mean ± SD. For sample characteristics see Table 1.

inhibition curves revealed that the conjugates were 1.4−2.7 times less toxic than free docetaxel when cells were incubated for a continuous 72 h (Table 2). HUVECs were more sensitive to docetaxel compared to prostate cancer cell lines as almost half of the drug concentrations were required to achieve the same magnitude of cell growth inhibition. Besides distinct difference between cytotoxic potential of free and conjugated forms of docetaxel, the difference between IC_{50} values for polymeric conjugates was found statistically insignificant ($p > 0.05$) for all cell lines tested.

Considering different routes of cellular entry and the necessity of lysosomal degradation of a linker between the polymer backbone and a drug, macromolecular therapeutics usually show 50−200-fold differences in the toxicity compare to a free drug.[17] The difference observed between IC_{50} values of free and conjugated forms of docetaxel was expected but was significantly smaller than that difference reported in the literature for other macromolecular therapeutics. It is possible that the hydrolysis of the ester bond and fast drug release from the conjugates are responsible for high toxicity of the conjugates. The same issue could play an important role in the efficacy of the conjugates in vivo as ester bonds could be cleaved by abundant esterases within the bloodstream.[61] In an attempt to mimic in vivo physiological conditions, DU145 cells in this study were exposed to the polymer−drug conjugates for 2 h, a time period relevant to the plasma half-life of typical HPMA copolymer−drug conjugates.[48] In these sets of experiments DU145 cells were exposed to the drugs for 2 h only and subsequently were washed with phosphate buffered saline, and incubation continued in

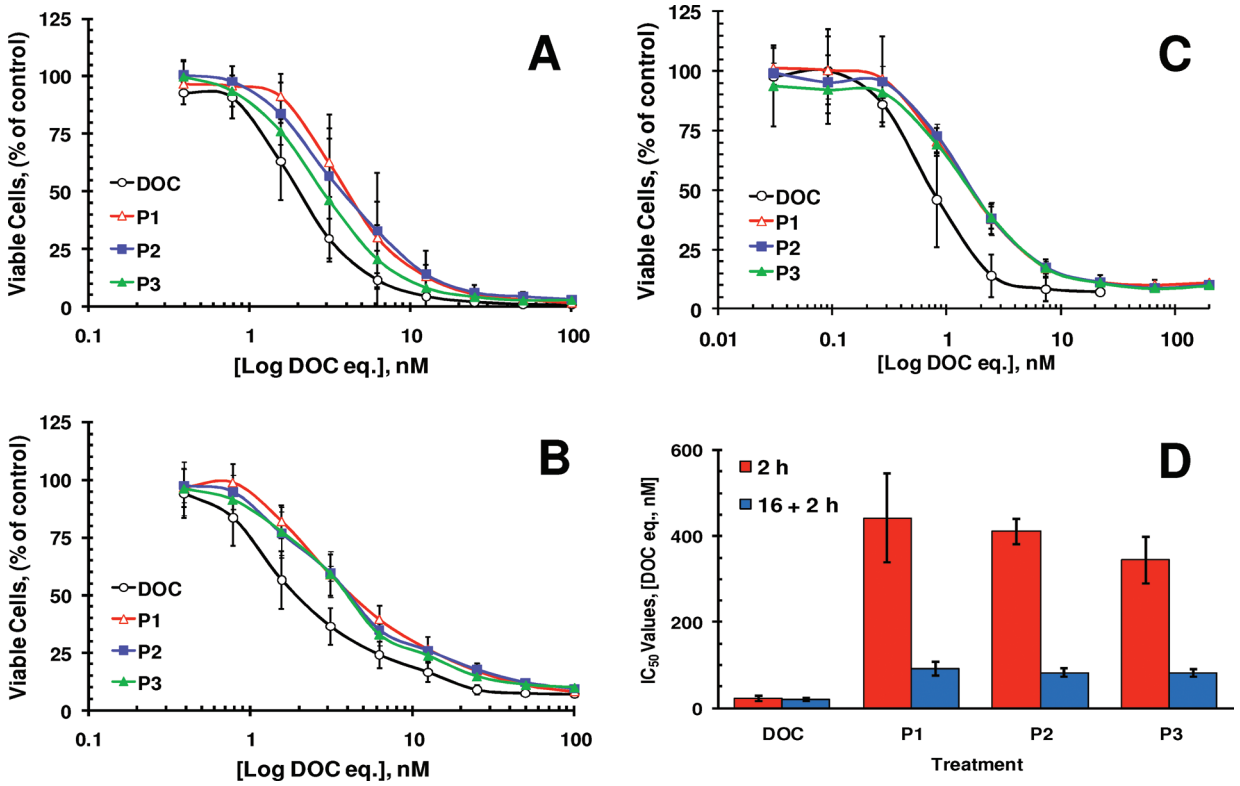

Figure 2. Toxicity of docetaxel conjugates toward cultured cells. DU145 (A), PC-3 (B) prostate cancer cells and HUVECs (C) were exposed to the compounds for a continuous 72 h. In pulse-chase experiments (D) DU145 cells were incubated with the compounds for 2 h only, washed with PBS and incubated in fresh growth medium for an additional 70 h. The legend for this plot indicates how long compounds were in contact with cell growth medium. All compounds were added to cells either immediately after dilution in cell growth medium (2 h) or after 16 h of preincubation in the same medium at 37 °C (16 + 2 h). The values of 3−4 independent experiments are presented as mean ± SD. For sample characteristics see Table 1.

Table 2. Calculated IC_{50} Values (nM)[a] after Continuous 72 h Incubation of Cells with Drugs

	DU145	PC-3	HUVEC
DOC	2.1 ± 0.5	1.8 ± 0.4	0.8 ± 0.1
P1	4.4 ± 1.1*	4.4 ± 0.7*	2.7 ± 0.9*
P2	3.0 ± 0.4*	4.3 ± 0.4*	2.3 ± 0.4*
P3	3.3 ± 0.8*	3.9 ± 0.7*	1.9 ± 0.5*

[a] *$p < 0.05$ vs DOC.

fresh growth medium without drugs until the number of cells was estimated. Therefore, this experimental setup allowed testing the influence of two important variables in these drug delivery systems: drug release rate and the presence of RGDfK targeting moiety. These experiments revealed a 15−20-fold difference between IC_{50} values of free and conjugated docetaxel when they were added to DU145 cells immediately after dilution in growth medium (Figure 2D). This difference is most likely due to the difference in the mechanisms of cellular internalization between two forms of the drug, because the stability studies performed with polymer−drug conjugates revealed that less than 3% docetaxel was released from polymer−drug conjugates in the presence of cell culture medium within 2 h (Figure 1). This suggested that the conjugates were not completely hydrolyzed within the first two hours. Prolonged 16 h preincubation of the conjugates in growth medium before the initiation of pulse-chase experiments significantly changed the observed difference between the two forms of doxorubicin (Figure 2D). After preincubation only 4−5-fold difference between IC_{50} values of free and conjugated docetaxel was observed most likely due to the release of the drugs from the conjugates. As in the experiments with 72 h continuous incubation, no statistically significant difference between IC_{50} values for the polymeric conjugates was found. Thus, given the two variables tested in this experiment, the release rate of free docetaxel proved to be the determinant variable that influenced the cytotoxicty of the tested constructs in vitro. High toxicity of the drug masked the binding advantage of the RGDfK moiety in vitro.

Competitive Binding Studies. Competitive binding studies demonstrated binding of the targeted HPMA copolymer−docetaxel−RGDfK conjugate (P2) to HUVEC and DU145 cell lines with IC_{50} values of 0.5 ± 0.2 μM and 2.6 ± 0.3 μM respectively (Figure 3). RGDfK peptide alone showed similar comparative binding affinities of 0.3 ± 0.1 μM and 1.5 ± 0.3 μM at equivalent peptide concentrations in HUVEC and DU145 cell lines. Untargeted conjugate (P1) was also evaluated in both cell lines and showed no evidence of active binding (Figure 3). These results demonstrate the ability of the targeted conjugate P2 (Table 1) to bind to $\alpha_v\beta_3$ integrins of HUVECs and DU145 cells. In both cases, conjugation of RGDfK to the HPMA copolymer backbone resulted in a small decrease in its binding affinity as compared to free RGDfK probably due to steric hindrance of the macromolecular system (Figure 3).

In Vivo Antitumor Efficacy of the Conjugates. One focus of this study was to evaluate whether the efficacy of macromolecules

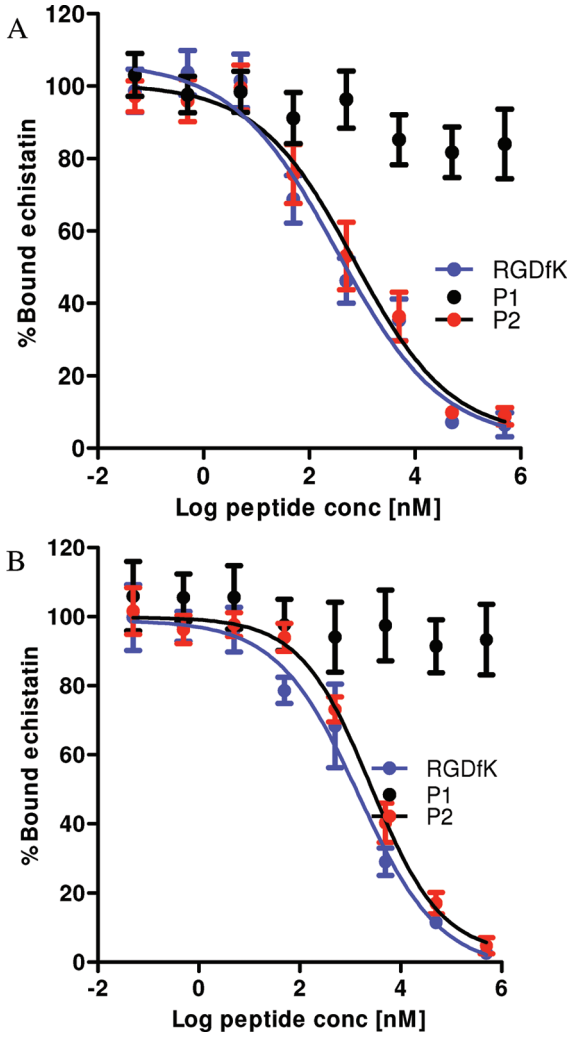

Figure 3. Competitive binding of HPMA copolymer conjugates and free RGDfK peptide binding of HPMA copolymer conjugates with and without RGDfK was compared to free peptide on (A) HUVEC and (B) human prostate cancer DU145 cells. Results are expressed as means of triplicate ± SD. For sample characteristics see Table 1.

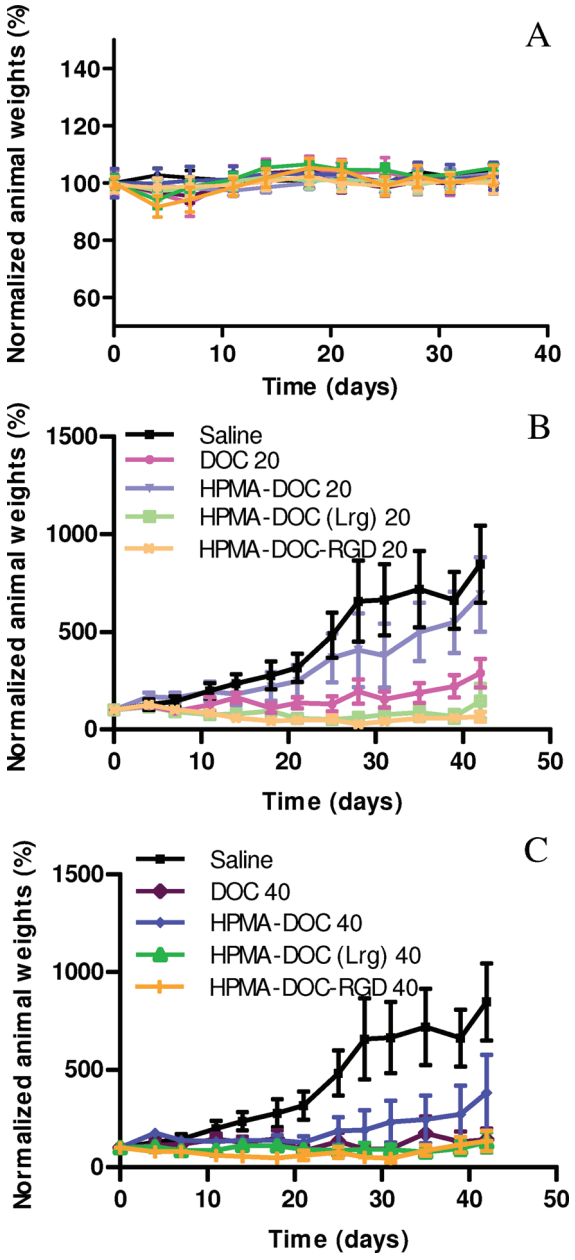

Figure 4. (A) Normalized animal weights as a function of time. Data are expressed as mean ± SEM (n = 5 per treatment group). (B) Efficacy of free drug and targeted/nontargeted polymer−drug conjugates P1, P2 and P3 at drug equivalent concentration of 20 mg/kg in nu/nu mice bearing DU145 tumor xenografts. (C) Efficacy of free drug and targeted/nontargeted polymer−drug conjugates P1, P2 and P3 at drug equivalent concentration of 40 mg/kg in nu/nu mice bearing DU145 tumor xenografts. Tumor volumes were normalized by their respective volume on day 0 (approx 50 mm^3). Data are expressed as mean ± SEM (n = 10 tumors per treatment group). For sample characteristics see Table 1.

with sizes below renal threshold can be enhanced by active targeting. To this end, we have chosen the cyclic integrin targeting peptide RGDfK as it has shown the ability to substantially increase tumor accumulation of HPMA copolymers in prostate tumors.[51] Docetaxel was chosen as it is the preferred drug of choice for patients with metastatic hormone refractive prostate cancer.[9] Efficacy of the conjugates was evaluated in nu/nu mice bearing DU145 prostate tumor xenografts. A single dose of each conjugate, free docetaxel, or control was administered. Physiological saline was used as a negative control and free docetaxel as positive control. The dose selection for both free drug and polymeric conjugates was 20 mg/kg and 40 mg/kg docetaxel equivalent, which corresponds to 60 mg/m^2 and 120 mg/m^2 in humans weighing 65 kg, as per calculation factors shown in the literature.[62,63] This dose was based on several phase II/III clinical trials[4,64−72] using docetaxel as a single agent as well as in combination chemotherapy, where doses varied between 30 mg/m^2 and 75 mg/m^2 given over several cycles.

Animals injected with free docetaxel at both 20 mg/kg and 40 mg/kg showed signs of hyperacute toxicity as they were rendered immobile for the first 30 min post injection. The lethargy shown by animals injected with free docetaxel was most likely a result of toxicity associated with the drug as well as the polysorbate 80 required to dissolve the drug for iv injection. None of the animals in the control group or those treated with conjugates showed any signs of acute toxicity. Mouse weights were followed up through the duration of the study as an overall measurement of the safety

of administered compounds. The normalized weights of animals showed no statistical difference between all groups for the duration of study (Figure 4A). Animals injected with free docetaxel showed statistically significant 2.6- and 2.9-fold reduction in mean tumor size as compared to saline at concentrations of 20 mg/kg ($P < 0.01$) and 40 mg/kg ($P < 0.001$). Although conjugate P1 (untargeted, low molecular weight HPMA−docetaxel) at 20 mg/kg demonstrated a 0.9-fold difference in mean tumor size as compared to saline, this difference was not statistically significant ($P > 0.1$). However, treatment animals with P1 at 40 mg/kg resulted in a 2.3-fold reduction in mean tumor size as compared to saline ($P < 0.05$).

Conjugate P2 (RGDfK targeted, low molecular weight HPMA copolymer−docetaxel) and conjugate P3 (untargeted, high molecular weight HPMA copolymer−docetaxel) at injected doses of 20 mg/kg and 40 mg/kg showed reductions in mean tumor size as compared to saline ($P < 0.001$) of 3.3-, 3.2-, 3.5-, and 3.4-fold respectively. While animals injected with both conjugates P2 and P3 demonstrated reduction in tumor size greater than the group injected with free docetaxel, only results with P2 at both 20 mg/kg and 40 mg/kg were statistically significant. The efficacy of P1 at 20 mg/kg was statistically inferior to that of P2 at 20 mg/kg and 40 mg/kg ($P < 0.01$) and that of P3 at doses of 20 mg/kg and 40 mg/kg ($P < 0.05$) with a mean difference in tumor size of 2.5-, 2.4-, 2.3-, and 2.2-fold. P1 at 40 mg/kg had no statistical difference in mean tumor size with P2 and P3 at 20 mg/kg and 40 mg/kg. P2 and P3 had no statistical difference at doses of 20 mg/kg or 40 mg/kg.

The lack of efficacy for P1 at 20 mg/kg in spite of efficacy observed in free docetaxel can be explained below: (i) low molecular weight P1 with a hydrodynamic diameter of 3.0 nm was small enough to be rapidly eliminated by glomerular filtration, thereby minimizing the persistence time of the conjugate in blood circulation which is necessary to achieve tumor accumulation due to the EPR effect, and/or (ii) the release of docetaxel from the conjugate was not fast enough for it to be effective prior to its elimination. Therefore, free docetaxel at this concentration was more effective than the untargeted low molecular weight conjugate. The efficacy of P1 was evident at 40 mg/kg because sufficient docetaxel could be released from the conjugate prior to elimination. The only advantage shown by animals injected with P1 was the lack of adverse hyperacute reaction in response to injection that was observed for free docetaxel administration, possibly due to the aqueous solubility acquired by polymer conjugation.

At 20 mg/kg, P2 showed the largest difference in tumor size with saline. Conjugate P2, like P1, had a hydrodynamic diameter of 3.0 nm, which was well below the glomerular renal threshold. The activity observed in these conjugates most probably is a consequence of active targeting as they had $\alpha_v\beta_3$ integrin targeting peptide RGDfK linked to the polymer side chains, thereby allowing them to anchor onto the neovasculature of angiogenic blood vessels. The RGD peptides have also been reported to be tumor penetrating, and its coadministration enhances the efficacy of anticancer drugs.[47] RGDfK in conjugate P2 may have also contributed to a greater efficacy. Conjugate P3, on the other hand, had a hydrodynamic diameter of 7.6 nm, which was above the glomerular renal threshold. This increases the plasma half-life and improves efficacy by passive targeting via the EPR effect. Administration of P3 at concentrations of 20 mg/kg had a reduction in mean tumor size difference as compared to saline ($P < 0.001$) and P1 ($P < 0.05$). Again, the difference in activity at 20 mg/kg of P3 when compared to free docetaxel was not statistically significant for the study period of 42 days.

Further, when comparisons were made between active targeting (P2) and passive targeting via the EPR effect (P3) at drug equivalent concentrations of 20 mg/kg, though the mean difference in tumor size between the groups was not significant, the mean tumor size reduction was greater in the case of actively targeted P2 conjugates. However at 40 mg/kg, which corresponds to 120 mg/m^2 in humans and is more than 1.5 times the highest concentration administered in clinical trials of docetaxel for treatment of prostate cancer, free drug and all three conjugates P1, P2 and P3 induced statistically significant tumor size reduction as compared to saline. The efficacy of P1 was evident at 40 mg/kg because sufficient docetaxel was released from the conjugate prior to elimination. Administrations of all three conjugates, unlike free docetaxel, demonstrated no visible signs of toxicity, and were freely soluble in saline.

The post hoc analysis of the variance of the mean size of the tumor over the entire study period of 42 days classified the conjugates and controls into three categories, i.e. those with high activity, those with moderate activity and those with no activity. Each compound falls under one or two categories. According to this analysis, saline falls in the low activity category, P1 at 20 mg/kg falls under the low and moderate activity categories, P1 at 40 mg/kg and free docetaxel at both 20 mg/kg and 40 mg/kg doses fall under moderate and high activity categories, and P2 and P3 at both 20 mg/kg and 40 mg/kg fall under the high activity category.

To summarize, administrations of all three conjugates, unlike free docetaxel, demonstrated no visible signs of toxicity, and were freely soluble in saline. Actively targeted conjugate P2 demonstrated the highest tumor size reduction for the duration of the study as compared to free docetaxel, small nontargeted conjugate P1 and passively targeted (via EPR) high molecular weight conjugate P3. All three conjugates were soluble in aqueous media and did not show any visible signs of hyperacute toxicity in animals. Further, while P3 does not have a biodegradable polymer backbone which would result in accumulation of the macromolecule post treatment, P2 has the advantage of a small size (3.0 nm), which can allow the dose fraction that does not reach the tumor to be eliminated.

■ CONCLUSIONS

HPMA copolymer−docetaxel conjugates with sizes of 3.0 and 7.6 nm, which correspond to dimensions below and above the glomular renal threshold, as well as $\alpha_v\beta_3$ integrin targeting conjugate HPMA copolymer−docetaxel−RGDfK of hydrodynamic diameter 3.0 nm, were successfully synthesized to evaluate the effect of active targeting with passive targeting. All the conjugates inhibited proliferation of human prostate cancer DU145 and PC3 cells as well as HUVEC at nanomolar concentrations. Cytotoxicity experiments by pulse-chase method where the incubation time with free drug and conjugates was limited to 2 h resulted in a 15−20-fold difference in activity of conjugates as compared to free docetaxel. This suggests that the conjugates were not completely hydrolyzed within the first two hours. Animals showed no visible signs of toxicity when injected with conjugates. HPMA copolymer−docetaxel conjugates of hydrodynamic diameter 7.6 nm and HPMA copolymer−docetaxel−RGDfK of hydrodynamic diameter 3.0 nm demonstrated the greatest tumor reduction capability with statistically

significant tumor regression compared to saline. Overall, the results demonstrate that $\alpha_v\beta_3$ integrin targeted low molecular weight conjugates with improved water solubility, reduced toxicity and ease of elimination post treatment in vivo are promising candidates for prostate cancer therapy.

AUTHOR INFORMATION

Corresponding Author

*Departments of Pharmaceutics & Pharmaceutical Chemistry and of Bioengineering, Utah Center for Nanomedicine, Nano Institute of Utah, University of Utah, 383 Colorow Road, Room 343, Salt Lake City, UT 84108, USA. Tel: (801) 587-1566. Fax: (801) 585-0575. E-mail: hamid.ghandehari@pharm.utah.edu.

Author Contributions

§These authors contributed equally to this work

ACKNOWLEDGMENT

This research was supported by the National Institutes of Health Grant R01 EB007171 and the Utah Science Technology and Research (USTAR) initiative.

REFERENCES

(1) Jemal, A.; Siegel, R.; Ward, E.; Hao, Y.; Xu, J.; Thun, M. J. Cancer statistics, 2009. *CA—Cancer J. Clin.* **2009**, *59* (4), 225–49.

(2) Mazhar, D.; Waxman, J. Early chemotherapy in prostate cancer. *Nat. Clin. Pract. Urol.* **2008**, *5* (9), 486–93.

(3) Petrylak, D. P.; Tangen, C. M.; Hussain, M. H.; Lara, P. N., Jr.; Jones, J. A.; Taplin, M. E.; Burch, P. A.; Berry, D.; Moinpour, C.; Kohli, M.; Benson, M. C.; Small, E. J.; Raghavan, D.; Crawford, E. D. Docetaxel and estramustine compared with mitoxantrone and prednisone for advanced refractory prostate cancer. *N. Engl. J. Med.* **2004**, *351* (15), 1513–20.

(4) Tannock, I. F.; de Wit, R.; Berry, W. R.; Horti, J.; Pluzanska, A.; Chi, K. N.; Oudard, S.; Theodore, C.; James, N. D.; Turesson, I.; Rosenthal, M. A.; Eisenberger, M. A. Docetaxel plus prednisone or mitoxantrone plus prednisone for advanced prostate cancer. *N. Engl. J. Med.* **2004**, *351* (15), 1502–12.

(5) Montero, A.; Fossella, F.; Hortobagyi, G.; Valero, V. Docetaxel for treatment of solid tumours: a systematic review of clinical data. *Lancet Oncol.* **2005**, *6* (4), 229–39.

(6) Ringel, I.; Horwitz, S. B. Studies with RP 56976 (taxotere): a semisynthetic analogue of taxol. *J. Natl. Cancer Inst.* **1991**, *83* (4), 288–91.

(7) Katsumata, N. Docetaxel: an alternative taxane in ovarian cancer. *Br. J. Cancer* **2003**, *89* (Suppl 3), S9–S15.

(8) Hotchkiss, K. A.; Ashton, A. W.; Mahmood, R.; Russell, R. G.; Sparano, J. A.; Schwartz, E. L. Inhibition of endothelial cell function in vitro and angiogenesis in vivo by docetaxel (Taxotere): association with impaired repositioning of the microtubule organizing center. *Mol. Cancer Ther.* **2002**, *1* (13), 1191–200.

(9) Shelley, M.; Harrison, C.; Coles, B.; Stafforth, J.; Wilt, T.; Mason, M. Chemotherapy for hormone-refractory prostate cancer. *Cochrane Database Syst. Rev.* **2006**, No. 4, No. CD005247.

(10) Leimgruber, K.; Negro, R.; Baier, S.; Moser, B.; Resch, G.; Sansone, S.; Adami, M.; Zanon, P.; Graiff, C.; Egarter-Vigl, E.; Wiedermann, C. J. Fatal interstitial pneumonitis associated with docetaxel administration in a patient with hormone-refractory prostate cancer. *Tumori* **2006**, *92* (6), 542–4.

(11) Engels, F. K.; Mathot, R. A.; Verweij, J. Alternative drug formulations of docetaxel: a review. *Anticancer Drugs* **2007**, *18* (2), 95–103.

(12) Kopecek, J.; Kopeckova, P.; Minko, T.; Lu, Z. HPMA copolymer-anticancer drug conjugates: design, activity, and mechanism of action. *Eur. J. Pharm. Biopharm.* **2000**, *50* (1), 61–81.

(13) Duncan, R. The dawning era of polymer therapeutics. *Nat. Rev. Drug Discovery* **2003**, *2* (5), 347–60.

(14) Matsumura, Y.; Maeda, H. A new concept for macromolecular therapeutics in cancer chemotherapy: mechanism of tumoritropic accumulation of proteins and the antitumor agent smancs. *Cancer Res.* **1986**, *46* (12 Part 1), 6387–92.

(15) Maeda, H.; Wu, J.; Sawa, T.; Matsumura, Y.; Hori, K. Tumor vascular permeability and the EPR effect in macromolecular therapeutics: a review. *J. Controlled Release* **2000**, *65* (1−2), 271–84.

(16) Noguchi, Y.; Wu, J.; Duncan, R.; Strohalm, J.; Ulbrich, K.; Akaike, T.; Maeda, H. Early phase tumor accumulation of macromolecules: A great difference in clearance rate between tumor and normal tissues. *Cancer Sci.* **1998**, *89* (3), 307–14.

(17) Kopecek, J.; Kopeckova, P. HPMA copolymers: origins, early developments, present, and future. *Adv. Drug Delivery Rev.* **2010**, *62* (2), 122–49.

(18) Rihova, B.; Bilej, M.; Vetvicka, V.; Ulbrich, K.; Strohalm, J.; Kopecek, J.; Duncan, R. Biocompatibility of N-(2-hydroxypropyl) methacrylamide copolymers containing adriamycin. Immunogenicity, and effect on haematopoietic stem cells in bone marrow in vivo and mouse splenocytes and human peripheral blood lymphocytes in vitro. *Biomaterials* **1989**, *10* (5), 335–42.

(19) Nishikawa, M.; Takakura, Y.; Hashida, M. Pharmacokinatic evaluation of polymeric carriers. *Adv. Drug Delivery Rev* **1996**, *21*, 135–55.

(20) Takakura, Y.; Fujita, T.; Hashida, M.; Sezaki, H. Disposition characteristics of macromolecules in tumor-bearing mice. *Pharm. Res.* **1990**, *7*, 339–46.

(21) Takakura, Y.; Hashida, M. Macromolecular carrier systems for targeted drug delivery: pharmacokinetic considerations on biodistribution. *Pharm. Res.* **1996**, *13*, 820–31.

(22) Takakura, Y.; Mahato, R. I.; Nishikawa, M.; Hashida, M. Control of pharmacokinetic profiles of drug-macromolecule conjugates. *Adv. Drug Delivery Rev.* **1996**, *19*, 377–99.

(23) Boucher, Y.; Baxter, L. T.; Jain, R. K. Interstitial pressure gradients in tissue-isolated and subcutaneous tumors: implications for therapy. *Cancer Res.* **1990**, *50* (15), 4478–84.

(24) Jain, R. K. Transport of molecules in the tumor interstitium: a review. *Cancer Res.* **1987**, *47* (12), 3039–51.

(25) Jain, R. K. Normalization of tumor vasculature: an emerging concept in antiangiogenic therapy. *Science* **2005**, *307* (5706), 58–62.

(26) Carmeliet, P.; Jain, R. K. Angiogenesis in cancer and other diseases. *Nature* **2000**, *407* (6801), 249–57.

(27) Yancopoulos, G. D.; Davis, S.; Gale, N. W.; Rudge, J. S.; Wiegand, S. J.; Holash, J. Vascular-specific growth factors and blood vessel formation. *Nature* **2000**, *407* (6801), 242–8.

(28) Leunig, M.; Yuan, F.; Menger, M. D.; Boucher, Y.; Goetz, A. E.; Messmer, K.; Jain, R. K. Angiogenesis, microvascular architecture, microhemodynamics, and interstitial fluid pressure during early growth of human adenocarcinoma LS174T in SCID mice. *Cancer Res.* **1992**, *52* (23), 6553–60.

(29) Yuan, F.; Salehi, H. A.; Boucher, Y.; Vasthare, U. S.; Tuma, R. F.; Jain, R. K. Vascular permeability and microcirculation of gliomas and mammary carcinomas transplanted in rat and mouse cranial windows. *Cancer Res.* **1994**, *54* (17), 4564–8.

(30) Kamoun, W. S.; Chae, S. S.; Lacorre, D. A.; Tyrrell, J. A.; Mitre, M.; Gillissen, M. A.; Fukumura, D.; Jain, R. K.; Munn, L. L. Simultaneous measurement of RBC velocity, flux, hematocrit and shear rate in vascular networks. *Nat. Methods* **2010**, *7* (8), 655–60.

(31) Endrich, B.; Reinhold, H. S.; Gross, J. F.; Intaglietta, M. Tissue perfusion inhomogeneity during early tumor growth in rats. *J. Natl. Cancer Inst.* **1979**, *62* (2), 387–95.

(32) Boucher, Y.; Jain, R. K. Microvascular pressure is the principal driving force for interstitial hypertension in solid tumors: implications for vascular collapse. *Cancer Res.* **1992**, *52* (18), 5110–4.

(33) Boucher, Y.; Leunig, M.; Jain, R. K. Tumor angiogenesis and interstitial hypertension. *Cancer Res.* **1996**, *56* (18), 4264–6.
(34) Jain, R. K.; Stylianopoulos, T. Delivering nanomedicine to solid tumors. *Nat. Rev. Clin. Oncol.* **2010**, *7* (11), 653–64.
(35) Nori, A.; Kopecek, J. Intracellular targeting of polymer-bound drugs for cancer chemotherapy. *Adv. Drug Delivery Rev.* **2005**, *57* (4), 609–36.
(36) Pasqualini, R.; Koivunen, E.; Ruoslahti, E. Alpha v integrins as receptors for tumor targeting by circulating ligands. *Nat. Biotechnol.* **1997**, *15* (6), 542–6.
(37) Koivunen, E.; Wang, B.; Ruoslahti, E. Phage libraries displaying cyclic peptides with different ring sizes: ligand specificities of the RGD-directed integrins. *Biotechnology (N.Y.)* **1995**, *13* (3), 265–70.
(38) Schraa, A. J.; Kok, R. J.; Moorlag, H. E.; Bos, E. J.; Proost, J. H.; Meijer, D. K. F.; de Leij, L.; Molema, G. Targeting of RGD-modified proteins to tumor vasculature: A pharmacokinetic and cellular distribution study. *Int. J. Cancer* **2002**, *102* (5), 469–475.
(39) Dubey, P. K.; Mishra, V.; Jain, S.; Mahor, S.; Vyas, S. P. Liposomes modified with cyclic RGD peptide for tumor targeting. *J. Drug Targeting* **2004**, *12* (5), 257–64.
(40) Koning, G. A.; Fretz, M. M.; Woroniecka, U.; Storm, G.; Krijger, G. C. Targeting liposomes to tumor endothelial cells for neutron capture therapy. *Appl. Radiat. Isot.* **2004**, *61* (5), 963–7.
(41) Schiffelers, R. M.; Koning, G. A.; ten Hagen, T. L.; Fens, M. H.; Schraa, A. J.; Janssen, A. P.; Kok, R. J.; Molema, G.; Storm, G. Anti-tumor efficacy of tumor vasculature-targeted liposomal doxorubicin. *J. Controlled Release* **2003**, *91* (1−2), 115–22.
(42) Chen, X.; Park, R.; Shahinian, A. H.; Bading, J. R.; Conti, P. S. Pharmacokinetics and tumor retention of 125I-labeled RGD peptide are improved by PEGylation. *Nucl. Med. Biol.* **2004**, *31* (1), 11–9.
(43) Meyer, A.; Auernheimer, J.; Modlinger, A.; Kessler, H. Targeting RGD recognizing integrins: drug development, biomaterial research, tumor imaging and targeting. *Curr. Pharm. Des.* **2006**, *12* (22), 2723–47.
(44) Ruoslahti, E. Specialization of tumour vasculature. *Nat. Rev. Cancer* **2002**, *2* (2), 83–90.
(45) Hajitou, A. Targeted systemic gene therapy and molecular imaging of cancer contribution of the vascular-targeted AAVP vector. *Adv. Genet.* **2010**, *69*, 65–82.
(46) Jiang, H.; Gomez-Manzano, C.; Lang, F. F.; Alemany, R.; Fueyo, J. Oncolytic adenovirus: preclinical and clinical studies in patients with human malignant gliomas. *Curr. Gene Ther.* **2009**, *9* (5), 422–7.
(47) Sugahara, K. N.; Teesalu, T.; Karmali, P. P.; Kotamraju, V. R.; Agemy, L.; Greenwald, D. R.; Ruoslahti, E. Coadministration of a tumor-penetrating peptide enhances the efficacy of cancer drugs. *Science* **2010**, *328* (5981), 1031–5.
(48) Borgman, M. P.; Aras, O.; Geyser-Stoops, S.; Sausville, E. A.; Ghandehari, H. Biodistribution of HPMA copolymer-aminohexylgeldanamycin-RGDfK conjugates for prostate cancer drug delivery. *Mol. Pharmaceutics* **2009**, *6* (6), 1836–47.
(49) Borgman, M. P.; Ray, A.; Kolhatkar, R. B.; Sausville, E. A.; Burger, A. M.; Ghandehari, H. Targetable HPMA Copolymer-Aminohexylgeldanamycin Conjugates for Prostate Cancer Therapy. *Pharm. Res.* **2009**, *6*, 1407–18.
(50) Mitra, A.; Coleman, T.; Borgman, M.; Nan, A.; Ghandehari, H.; Line, B. R. Polymeric conjugates of mono- and bi-cyclic alphaVbeta3 binding peptides for tumor targeting. *J. Controlled Release* **2006**, *114* (2), 175–83.
(51) Pike, D. B.; Ghandehari, H. HPMA copolymer-cyclic RGD conjugates for tumor targeting. *Adv. Drug Delivery Rev.* **2010**, *62* (2), 167–83.
(52) Zarabi, B.; Borgman, M. P.; Zhuo, J.; Gullapalli, R.; Ghandehari, H. Noninvasive monitoring of HPMA copolymer-RGDfK conjugates by magnetic resonance imaging. *Pharm. Res.* **2009**, *26* (5), 1121–9.
(53) Hood, J. D.; Cheresh, D. A. Role of integrins in cell invasion and migration. *Nat. Rev. Cancer* **2002**, *2* (2), 91–100.
(54) Greish, K.; Ray, A.; Bauer, H.; Larson, N.; Malugin, A.; Pike, D.; Haider, M.; Ghandehari, H. Anticancer and antiangiogenic activity of HPMA copolymer-aminohexylgeldanamycin-RGDfK conjugates for prostate cancer therapy. *J. Controlled Release* **2011**, *151* (3), 263–70.
(55) Strohalm, J.; Kopecek, J. Poly *N*-(2-hydroxypropyl) methacrylamide: 4. Heterogenous polymerization. *Angew. Makromol. Chem.* **1978**, *70*, 109–18.
(56) Rejmanova, P.; Labsky, J.; Kopecek, J. Aminolyses of monomeric and polymeric p-nitrophenyl esters of methacryloylated amino acids. *Makromol. Chem.* **1977**, *178*, 2159–68.
(57) Ulbrich, K.; Subr, V.; Strohalm, J.; Plocova, D.; Jelinkova, M.; Rihova, B. Polymeric drugs based on conjugates of synthetic and natural macromolecules. I. Synthesis and physico-chemical characterisation. *J. Controlled Release* **2000**, *64* (1−3), 63–79.
(58) Lee, J. H.; Kopeckova, P.; Kopecek, J.; Andrade, J. D. Surface properties of copolymers of alkyl methacrylates with methoxy (polyethylene oxide) methacrylates and their application as protein-resistant coatings. *Biomaterials* **1990**, *11* (7), 455–64.
(59) Ulbrich, K.; Zacharieva, E. I.; Obereigner, B.; Kopecek, J. Polymers containing enzymatically degradable bonds V. Hydrophilic polymers degradable by papain. *Biomaterials* **1980**, *1* (4), 199–204.
(60) Baltes, T.; Garret-Flaudy, F.; Freitag, R. Investigation of the LCST of polyacrylamides as a function of molecular parameters and the solvent composition. *J. Polym. Sci., Part A: Polym. Chem.* **1999**, *37* (15), 2977–89.
(61) Liederer, B. M.; Borchardt, R. T. Enzymes involved in the bioconversion of ester-based prodrugs. *J. Pharm. Sci.* **2006**, *95* (6), 1177–95.
(62) Freireich, E. J.; Gehan, E. A.; Rall, D. P.; Schmidt, L. H.; Skipper, H. E. Quantitative comparison of toxicity of anticancer agents in mouse, rat, hamster, dog, monkey, and man. *Cancer Chemother. Rep.* **1966**, *50* (4), 219–44.
(63) Reagan-Shaw, S.; Nihal, M.; Ahmad, N. Dose translation from animal to human studies revisited. *FASEB J.* **2008**, *22* (3), 659–61.
(64) Picus, J.; Schultz, M. Docetaxel (Taxotere) as monotherapy in the treatment of hormone-refractory prostate cancer: preliminary results. *Semin. Oncol.* **1999**, *26* (5 Suppl. 17), 14–8.
(65) Friedland, D.; Cohen, J.; Miller, R., Jr.; Voloshin, M.; Gluckman, R.; Lembersky, B.; Zidar, B.; Keating, M.; Reilly, N.; Dimitt, B. A phase II trial of docetaxel (Taxotere) in hormone-refractory prostate cancer: correlation of antitumor effect to phosphorylation of Bcl-2. *Semin. Oncol.* **1999**, *26* (5 Suppl. 17), 19–23.
(66) Berry, W.; Dakhil, S.; Gregurich, M. A.; Asmar, L. Phase II trial of single-agent weekly docetaxel in hormone-refractory, symptomatic, metastatic carcinoma of the prostate. *Semin. Oncol.* **2001**, *28* (4 Suppl. 15), 8–15.
(67) Beer, T. M.; Pierce, W. C.; Lowe, B. A.; Henner, W. D. Phase II study of weekly docetaxel in symptomatic androgen-independent prostate cancer. *Ann. Oncol.* **2001**, *12* (9), 1273–9.
(68) Gravis, G.; Bladou, F.; Salem, N.; Macquart-Moulin, G.; Serment, G.; Camerlo, J.; Genre, D.; Bardou, V. J.; Maraninchi, D.; Viens, P. Weekly administration of docetaxel for symptomatic metastatic hormone-refractory prostate carcinoma. *Cancer* **2003**, *98* (8), 1627–34.
(69) Petrylak, D. P. Docetaxel for the treatment of hormone-refractory prostate cancer. *Rev. Urol.* **2003**, *5* (Suppl. 2), S14–21.
(70) Petrylak, D. P.; Ankerst, D. P.; Jiang, C. S.; Tangen, C. M.; Hussain, M. H.; Lara, P. N., Jr.; Jones, J. A.; Taplin, M. E.; Burch, P. A.; Kohli, M.; Benson, M. C.; Small, E. J.; Raghavan, D.; Crawford, E. D. Evaluation of prostate-specific antigen declines for surrogacy in patients treated on SWOG 99-16. *J. Natl. Cancer Inst.* **2006**, *98* (8), 516–21.
(71) Sinibaldi, V. J.; Carducci, M. A.; Moore-Cooper, S.; Laufer, M.; Zahurak, M.; Eisenberger, M. A. Phase II evaluation of docetaxel plus one-day oral estramustine phosphate in the treatment of patients with androgen independent prostate carcinoma. *Cancer* **2002**, *94* (5), 1457–65.
(72) Savarese, D. M.; Halabi, S.; Hars, V.; Akerley, W. L.; Taplin, M. E.; Godley, P. A.; Hussain, A.; Small, E. J.; Vogelzang, N. J. Phase II study of docetaxel, estramustine, and low-dose hydrocortisone in men with hormone-refractory prostate cancer: a final report of CALGB 9780. Cancer and Leukemia Group B. *J. Clin. Oncol.* **2001**, *19* (9), 2509–16.